DOI: 10.1021/ma102702a

Macromolecules
ARTICLE

Optically Active Amphiphilic Polymer Brushes Based on Helical Polyacetylenes: Preparation and Self-Assembly into Core/Shell Particles

Lei Ding, Yingying Huang, Yuanyuan Zhang, Jianping Deng,* and Wantai Yang

State Key Laboratory of Chemical Resource Engineering, Beijing University of Chemical Technology, Beijing 100029, China, and College of Materials Science and Engineering, Beijing University of Chemical Technology, Beijing 100029, China

Received November 26, 2010; Revised Manuscript Received January 14, 2011

ABSTRACT: The article reports on the first preparation and self-assembly of a unique class of amphiphilic polymer brushes, which consist of hydrophobic optically active helical polyacetylene backbones and hydrophilic thermosensitive poly(*N*,*N*-dimethylamino-2-ethyl methacrylate) (PDMAEMA) side chains. The polymer brushes were prepared by a two-step process: substituted acetylene monomers underwent catalytic copolymerizations to form optically active helical polymer backbones bearing −Br moieties in side chains, which were employed as macroinitiators for the subsequent atom transfer radical polymerization (ATRP) of a vinyl monomer DMAEMA. High specific rotations and intense circular dichroism effects demonstrated that the polymer brushes possessed optical activities, derived from the helical polyacetylene backbones. The polymer brushes could self-assemble in water/tetrahydrofuran mixture solvent to form core/shell structured nanoparticles, which showed considerable optical activity originated in the helical polyacetylene cores. The core/shell nanoparticles also exhibited thermosensitivity due to the PDMAEMA shells. This article thus provides an efficient approach for preparing novel optically active polymers and core/shell nanoparticles from helical polyacetylenes.

Introduction

Polymer brushes (PBs) as a unique class of polymeric architectures comprised of long backbones and densely grafted side chains have attracted ever-growing attention due to their unique structures, properties, and potential applications.[1,2] PBs can be prepared by three techniques:[3] "grafting through" (the polymerization of macromonomers),[3d] "grafting onto" (the addition of preprepared side chains to a backbone),[3a] and "grafting from" (the formation of side chains from a macroinitiator backbone),[3-b,c] among which the "grafting from" method is considered to be the most efficient for the synthesis of PBs with high grafting density and well-defined backbones and side chains.[1a] Many researchers made significant contributions toward the progress in the synthesis of PBs.[4] Meanwhile, PBs with either a helical polypeptide backbone or helical polypeptide side chains have also been extensively investigated in recent years.[5] However, in spite of the many PBs based on helical polypeptides, few reports were focused on the synthesis of PBs derived from artificially helical conjugated polymer main chains.[6] This article will report such a unique type of amphiphilic PBs consisting of hydrophobic helical polymer main chains and hydrophilic side chains and their self-assembly.

Conjugated polymers have been of increasing interest because of their intriguing properties and their potentials in electronic and photonic applications,[7] in particular after the 2001 Noble prize was awarded to Professors Heeger, McDiarmid, and Shirakawa.[8] Conjugated polymers which can adopt helical conformations are of fundamental importance for both scientific and applicative purposes.[9] We have prepared a series of substituted polyacetylenes adopting helical structures under suitable conditions, including poly(*N*-propargylamide)s,[10] poly(*N*-propargylsulfamide)s,[11] and poly(*N*-propargylurea)s.[12] Furthermore, optically active polymer nanoparticles[13] and core/shell nanoparticles[14] derived from helical substituted polyacetylenes were prepared via catalytic emulsion polymerizations in aqueous systems. Such optically active nanoparticles can also be prepared via emulsification of the preformed helical polymers.[15] In the present article, we will report for the first time another efficient approach, i.e., self-assembly of the polymer brushes, for the preparation of core/shell nanoparticles consisting of helical polyacetylenes and showing thermosensitivity, as will be described below.

In this article, the "grafting from" method was employed to prepare the designed PBs, which are composed of helical poly(*N*-propargylamide) main chains (also acting as macroinitiator for the subsequent ATRP) and thermosensitive poly(*N*,*N*-dimethylamino-2-ethyl methacrylate) (PDMAEMA) side chains. Such PBs were prepared by combining catalytic polymerization of substituted acetylene monomers (to form the helical macromolecular main chains) with ATRP technique of a vinyl monomer (DMAEMA, to form the side chains). The relevant strategy is schematically presented in Scheme 1. Apart from the interesting helical main chains and the optical activities, such PBs could self-assemble in water/THF (tetrahydrofuran) mixture solvent to form core/shell nanoparticles, which also exhibited considerable optical activities. Additionally, the shell-forming PDMAEMA chains rendered the expected thermosensitivity to the core/shell nanoparticles, indicating the intriguing potential applications of the present core/shell nanoparticles for instance in drug delivery, chiral recognition, chiral catalysis, and chiral sensors.

Experimental Part

Materials. The solvents were purified by distilling under reduced pressure prior to use. Rh catalyst $[(nbd)Rh^{+}B^{-}(C_6H_5)_4]$

*Corresponding author: Tel +86-10-6443-5128; Fax +86-10-6443-5128; e-mail dengjp@mail.buct.edu.cn.

 Published on Web 01/27/2011

Scheme 1. Schematic Representation for Preparing and Self-Assembly of Amphiphilic Optically Active Polymer Brushes

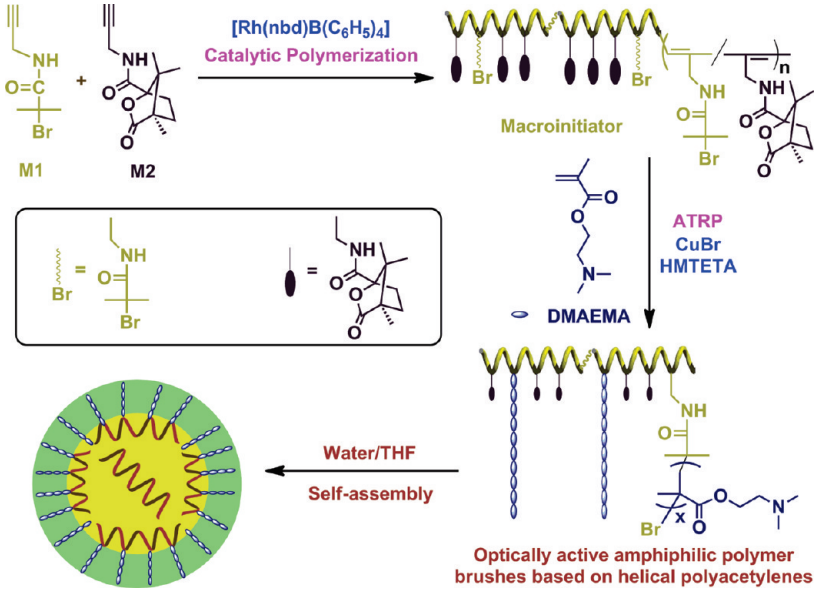

(nbd = norbornadiene) was prepared as reported.[16] The reagents were purchased from Aldrich, unless otherwise noted. *N*,*N*-Dimethylamino-2-ethyl methacrylate (DMAEMA) was used after removal of the inhibitors in a ready-to-use disposable inhibitor-removal column (Aldrich). Copper(I) bromide (CuBr) was washed with glacial acetic acid three times, dried in vacuum at room temperature, and then stored in an amber bottle. Propargylamine, 2-bromoisobutyric acid (Alfa Aesar), isobutyl chloroformate (Alfa Aesar), 4-methylmorpholine (Alfa Aesar), and 1,1,4,7,10,10-hexamethyltriethylenetetramine (HMTETA) were used as received without additional purification.

Measurements. ^{1}H and ^{13}C NMR spectra were recorded on a Bruker AV600 spectrometer with $CDCl_3$ as solvent. FT-IR spectra were recorded with a Nicolet Nexus 670 infrared spectrometer (KBr tablet). Elemental analysis was carried out on a Thermo EA 1112 elemental analyzer. UV−vis absorption and circular dichroism (CD) spectra were recorded in chloroform on a Jasco 810 spectropolarimeter. Number-average molecular weights (M_n) and molecular weight distributions (PDI, M_w/M_n) of the polymers were determined by GPC (Waters 515-2410 system) calibrated by using polystyrenes as the standards and THF as the eluent. Specific rotations were measured on a JASCO P-1020 digital polarimeter with a sodium lamp as the light source at room temperature. The morphology of the self-assembly products was observed on a Hitachi H-800 transmission electron microscope (TEM). The particle size and size distribution were determined by a laser particle size analyzer (ZETA SIZER Nano series, zen3600).

Synthesis of Monomers. M1 was synthesized as a new compound referring to the method introduced elsewhere.[10] The major synthetic procedure is described below. 2-Bromoisobutyric acid (4.87 g, 29.16 mmol), isobutyl chloroformate (3.78 mL, 29.16 mmol), and 4-methylmorpholine (3.2 mL, 29.16 mmol) were subsequentially added in THF (100 mL). The solution was stirred at ambient temperature for about 20 min, and then propargylamine (2 mL, 29.16 mmol) was added dropwise to the solution. The solution was stirred for another 5 h, and the white precipitate therein formed was filtered off. The filtrate was washed with 2 M HCl aqueous solution three times and then with saturated $NaHCO_3$ aqueous solution for neutralization. Afterward, the solution was dried over anhydrous $MgSO_4$, filtered, and concentrated to give the target monomer. The crude monomer was purified by flash column chromatography on silica gel (hexane/AcOEt = 3/1, v/v) to give a colorless liquid. After removing the solvent by rotary evaporator, **M1** in white crystal was obtained. The analytical and spectroscopic data of **M1** are as follows. Yield: 58%. FT-IR (KBr): 3299 (H−N), 2123 (H−C≡), 1660 (C=O), 1523, 585 cm^{-1} (C−Br). ^{1}H NMR ($CDCl_3$, 600 MHz, 20 °C): δ 2.16 (s, 1H, *CH*≡C), 3.89 (m, 2H, CH≡C−*CH*$_2$), 7.12 (s, 1H, *NH*), 1.79 ppm (s, 6H, C-(*CH*$_3$)$_2$Br). ^{13}C NMR ($CDCl_3$, 150 MHz, 20 °C): δ 27.8, 31.9, 60.2, 71.7, 79.2, 171.6 ppm. Elemental analysis calcd (%) for $C_7H_{10}BrNO$ (204.06): C 41.20, H 4.94, N 6.86; Found: C 41.29, H 4.85, N 6.90. The synthesis of **M2** was reported earlier.[17]

Synthesis of Macroinitiators via Catalytic Polymerization. Predetermined amounts of **M1** and **M2** copolymerized to provide the macroinitiators poly(**1**$_1$-*co*-**2**$_6$) and poly(**1**$_1$-*co*-**2**$_{10}$) bearing −Br moieties for the subsequent ATRP reactions. The copolymerizations were carried out with [(nbd)Rh$^+$B$^-$(C$_6$H$_5$)$_4$] as a catalyst in dry $CHCl_3$ under nitrogen at 30 °C for 5 h with [monomer]$_0$ = 1.0 M (total monomer concentration) and [catalyst] = 0.01 M. After polymerization, the solution containing the resulting polymer was poured into a large amount of hexane to precipitate the polymer. The polymer was filtered and then dried under reduced pressure.

Synthesis of Amphiphilic Polymer Brushes via ATRP. Polymer brushes (poly(**1**$_1$-*co*-**2**$_6$)-*g*-PDMAEMA and poly(**1**$_1$-*co*-**2**$_{10}$)-*g*-PDMAEMA) were synthesized using poly(**1**$_1$-*co*-**2**$_6$) and poly(**1**$_1$-*co*-**2**$_{10}$) obtained above as ATRP macroinitiators with molar feed ratio [DMAEMA]/[**M1**]/[CuBr]/[HMTETA] of 150/1/1/1.2. ATRP reaction was performed in a 25 mL Schlenk tube equipped with a magnetic stirrer, and the typical procedure is described below. Predetermined amounts of CuBr, DMAEMA, and HMTETA were added in the tube containing 2 mL of methanol/water (3/1, v/v) mixture. The reaction mixture was degassed by three vacuum/nitrogen cycles. Then a solution of macroinitiator in 3.5 mL of THF was introduced into the mixture under a dry nitrogen atmosphere. The tube was then sealed with a three-way stopcock, and the polymerization reaction was allowed to proceed under continuous stirring at 60 °C for 8 h. The reaction was stopped by diluting with THF, and the diluted mixture was passed through an activated basic aluminum oxide column to remove the catalyst complex. After removing most THF using a rotary evaporator and precipitating the solution in excess *n*-hexane, the product was collected by filtration and dried under vacuum at room temperature for 24 h. The obtained polymer brushes were subjected to ^{1}H NMR spectroscopy and GPC measurements.

Self-Assembly of Amphiphilic Polymer Brushes. Self-assembly of the amphiphilic polymer brushes was performed by dissolving

the polymer (10 mg) in THF (0.2 mL), followed by progressive addition (1 drop/10 s) of 1 mL of deionized water under vigorous stirring. A complete removal of THF was realized by spontaneous evaporation, and the self-assembly product was then subjected to CD and TEM measurements.

Results and Discussion

Strategy for the Preparation of Amphiphilic Polymer Brushes. The strategy for preparing the amphiphilic optically active polymer brushes based on helical polyacetylene is schematically presented in Scheme 1. A new *N*-propargylamide monomer (**M1**) containing a specially designed α-bromoisobutyryl group was synthesized referring to the method described earlier.[10] The polymer brushes were synthesized by combining two different polymerization mechanisms in a two-step process. In the first step, helical copolymers containing −Br moieties (microinitiators) were synthesized by catalytic copolymerization of **M1** with **M2** in the presence of $[(nbd)Rh^{+}B^{-}(C_6H_5)_4]$, which proved to be an efficient catalyst for preparing acetylene-based polymers with high stereoregularity.[10−12] In the second step, monomer DMAEMA underwent ATRP with the prepared helical copolymers as macroinitiators to yield the expected amphiphilic polymer brushes consisting of helical poly(*N*-propargylamide) main chains and thermosensitive PDMAEMA side chains. More interestingly, the amphiphilic polymer brushes also displayed considerable optical activity derived from the helical main chains and could self-assemble spontaneously in water/THF to form nanoparticles consisting of optically active cores and thermosensitive shells. Herein, it should be pointed out that the homopolymer from **M2** (poly-**2**) could adopt helical structures,[17] while **M1** also could provide the homopolymer (poly-**1**) adopting helical structures under suitable conditions, as will be discussed later on. The reason for using the copolymers from **M1** and **M2** as the macroinitiators for the subsequent ATRP lies in the observation that if poly-**1** was used as the macroinitiator, gels were frequently occurred after the ATRP reactions. This will be stated in detail below. In addition, chiral **M2** units in the copolymers rendered the expected optical activities.

Synthesis and (Co)polymerization of Monomers. M1 containing a α-bromoisobutyryl group was synthesized for the first time. The relevant synthesis, purification, and identification processes are described in the Experimental Part. A typical ^{1}H NMR spectrum is shown in Figure 1A. The characteristic resonances for all the protons of **M1** can be clearly observed at their corresponding positions as illustrated in the figure, demonstrating the successful preparation of **M1**. **M1** underwent homopolymerization smoothly in chloroform in the presence of Rh-based catalyst, providing the poly-**1** with moderate molecular weight (M_n = 7000, M_w/M_n = 1.60) in a high yield (97%). However, there is no chiral center in **M1**, so poly-**1** did not show any optical activity even though it could adopt helical conformations. This will be discussed in more detail below.

To prepare polymer brushes comprised of optically active helical polymeric main chains, **M2** was employed to carry out copolymerizations with **M1** since poly-**2** is known to adopt helical conformations and furthermore showed considerable optical activity.[17] On the other hand, it was reported that when ATRP is carried out from a macroinitiator with local highly concentrated initiation sites (−Br moieties), radical−radical coupling of the propagating chains will presumably occur and result in gelation.[18] This situation was also observed in our experiments. Accordingly, **M1** underwent copolymerizations with **M2** in two varied monomer feed

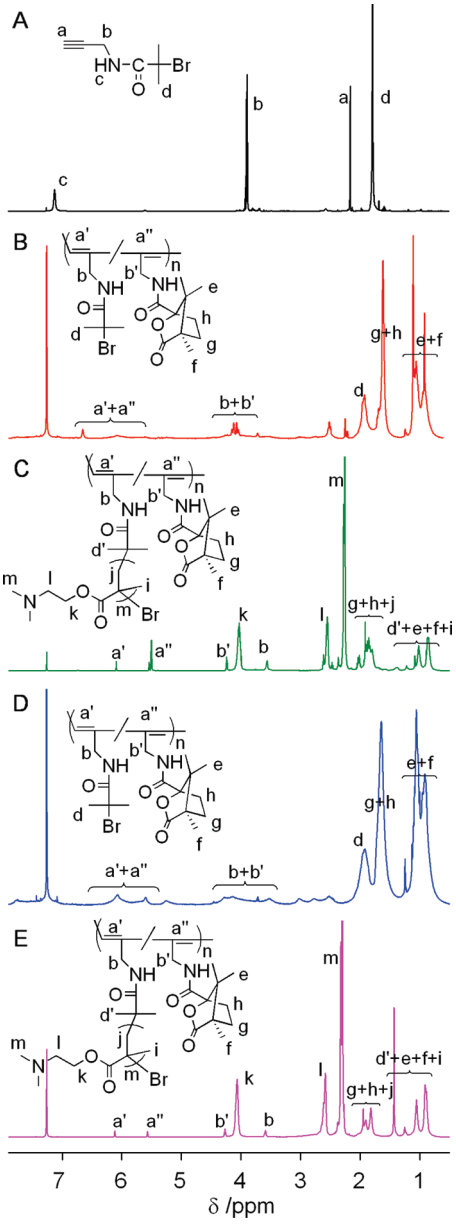

Figure 1. ^{1}H NMR spectra for (A) **M1**, (B) poly(**1**$_1$-*co*-**2**$_6$), (C) poly(**1**$_1$-*co*-**2**$_6$)-*g*- PDMAEMA8, (D) poly(**1**$_1$-*co*-**2**$_{10}$), and (E) poly(**1**$_1$-*co*-**2**$_{10}$)-*g*-PDMAEMA.

ratios (**M1**/**M2** = 1/6 and 1/10, in mol), yielding copolymers designated as poly(**1**$_1$-*co*-**2**$_6$) and poly(**1**$_1$-*co*-**2**$_{10}$), respectively. The copolymerzation results are presented in Table 1. The copolymers could be obtained with moderate molecular weights (M_n = 11 000 and 20 100) with a quantitative conversion (yield = 99% and 100%, respectively). The polydispersity indices (M_w/M_n) were 1.50 and 1.77, respectively. The GPC traces of poly(**1**$_1$-*co*-**2**$_6$) and poly(**1**$_1$-*co*-**2**$_{10}$) are depicted in Figure 2a,e. Taking into account the quantitative yields, it is reasonably assumed that the compositions of the copolymers were equal to the corresponding monomer feed ratios. This consideration is proved correct since the calculations by NMR technique gave the similar results (**M1** content: 14.5% in poly(**1**$_1$-*co*-**2**$_6$) and 9.4% in poly(**1**$_1$-*co*-**2**$_{10}$) (will be discussed in next paragraph). Also of particular importance is that both poly(**1**$_1$-*co*-**2**$_6$) and poly(**1**$_1$-*co*-**2**$_{10}$) displayed high specific rotations (−5548° and −9018°, Table 1), reflecting that the copolymers were optically active, just as expected. The optical activity resulted from the helical

Table 1. Data of Poly($\mathbf{1}_1$-*co*-$\mathbf{2}_6$) and Poly($\mathbf{1}_1$-*co*-$\mathbf{2}_{10}$)[a]

		copolymer					
macroinitiator	monomer ratio **M1**/**M2** (mol/mol)	yield (%)[b]	**M1** units content (%)[c]	M_n[d]	M_w/M_n[d]	$[\alpha]_D$ (deg)[e]	*g*-value (10^{-3})[f]
poly($\mathbf{1}_1$-*co*-$\mathbf{2}_6$)	1/6	99	14.5	11 000	1.50	−5548	−2.53
poly($\mathbf{1}_1$-*co*-$\mathbf{2}_{10}$)	1/10	100	9.4	20 100	1.77	−9018	−2.58

[a] With [(nbd)Rh$^+$B$^-$(C_6H_5)$_4$] as catalyst at 30 °C for 5 h; $[M]_0$ = 1 mol/L; $[M]_0$/[Rh] = 100; solvent, $CHCl_3$. [b] Hexane-insoluble part. [c] Determined by comparing the area ratio of the corresponding peaks (d/(g + h)) in the ^{1}H NMR spectra (see Figure 1B,D). [d] Measured by GPC, using polystyrene as the standard and THF as eluent. [e] Measured by polarimeter in $CHCl_3$ at room temperature (c = 0.085−0.1 g/dL). [f] *g*-value = $\Delta\varepsilon/\varepsilon$, in which $\Delta\varepsilon = [\theta]/3298$, temperature = 20 °C. The data of $\Delta\varepsilon$ and $[\theta]$ are based on Figure 4.

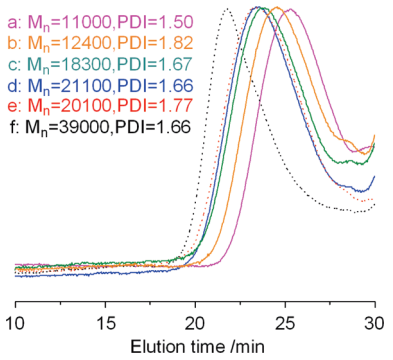

Figure 2. GPC traces of (a) poly($\mathbf{1}_1$-*co*-$\mathbf{2}_6$), (b) poly($\mathbf{1}_1$-*co*-$\mathbf{2}_6$)-*g*-PDMAEMA2, (c) poly($\mathbf{1}_1$-*co*-$\mathbf{2}_6$)-*g*-PDMAEMA4, (d) poly($\mathbf{1}_1$-*co*-$\mathbf{2}_6$)-*g*-PDMAEMA8, (e) poly($\mathbf{1}_1$-*co*-$\mathbf{2}_{10}$), and (f) poly($\mathbf{1}_1$-*co*-$\mathbf{2}_{10}$)-*g*-PDMAEMA.

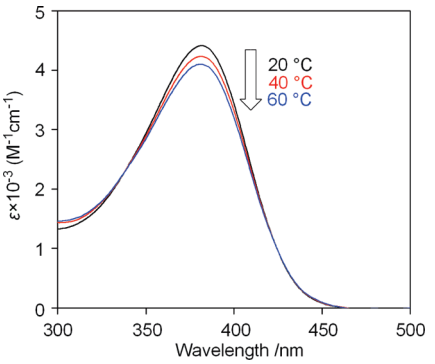

Figure 3. UV−vis spectra of poly-**1** measured at varied temperatures in $CHCl_3$ (c = 0.1 mM).

conformations of the copolymer backbones, which will be discussed below.

To further investigate the compositions of the as-prepared macroinitiators, poly($\mathbf{1}_1$-*co*-$\mathbf{2}_6$) and poly($\mathbf{1}_1$-*co*-$\mathbf{2}_{10}$) were subjected to ^{1}H NMR spectroscopy measurement, and the relevant results are presented in Figure 1B,D. The peaks located at chemical shifts of δ 5−7 ppm are attributable to the olefinic protons in the copolymer main chains. Reportedly, highly stereoregular poly(*N*-propargylamide)s frequently displayed a sharp signal at 5−7 ppm due to the olefinic protons in the main chains.[10−12] However, the peaks located at chemical shifts of 5−7 ppm in the present poly($\mathbf{1}_1$-*co*-$\mathbf{2}_6$) and poly($\mathbf{1}_1$-*co*-$\mathbf{2}_{10}$) were too broad, and so the stereoregularity of their main chains could not be determined. The signals located at chemical shifts in 3−5 ppm correspond to the methylene protons adjacent to C=C double bonds of the polymer backbones (b and b′, C=C−CH_2−NH). The chemical shifts associated with the methyl protons (e and f, −CH_3) derived from **M2** were located at 0.9−1.2 ppm. The signal at δ = 1.93 ppm is attributed to the methyl protons (d, −C(CH_3)$_2$Br) adjacent to bromide, which provides significant evidence for the incorporation of α-bromoisobutyrate moieties in the pendent groups of the copolymer. The peaks at chemical shifts of 1.5−1.8 ppm are associated with the methylene protons (g and h, C−CH_2CH_2−C) originating in **M2**. According to the peak area ratio of d/(g + h), the content of **M1** units in the copolymer was determined to be 14.5% in poly($\mathbf{1}_1$-*co*-$\mathbf{2}_6$) and 9.4% in poly($\mathbf{1}_1$-*co*-$\mathbf{2}_{10}$). This offers evident support for the assumption that the compositions of the copolymers were almost equal to the corresponding monomer feed ratios, as mentioned above.

Helical Structures of Poly($\mathbf{1}_1$-*co*-$\mathbf{2}_6$) and Poly($\mathbf{1}_1$-*co*-$\mathbf{2}_{10}$). Before exploring the helical structures of the copolymers, the secondary structure of poly-**1** was first investigated by UV−vis and CD spectroscopy measurements, which have been widely used in earlier investigations.[10−12] The UV−vis spectra of poly-**1** measured at varied temperatures in chloroform are presented in Figure 3. Poly-**1** showed a strong UV−vis absorption at ∼390 nm. This is in good agreement with the previous poly(*N*-propargylamide)s with similar structures and demonstrates that poly-**1** adopted helical conformations.[10] More importantly, the intensities of the UV−vis spectra of poly-**1** measured at different temperatures exhibited only slight differences, indicating that the helical structures in poly-**1** were rather stable in a temperature range from 20 to 60 °C. However, no CD signal was observed in the CD spectra of poly-**1** because it contained no chiral structure. Taking into consideration the helical structures of poly-**1** and poly-**2**,[17] it can be considered that the copolymer of **M1** and **M2** will in principle also form helical polymer backbones. This hypothesis is proved correct and will be discussed next.

The UV−vis and CD spectra of poly($\mathbf{1}_1$-*co*-$\mathbf{2}_6$) and poly($\mathbf{1}_1$-*co*-$\mathbf{2}_{10}$) are presented in Figure 4. As can be observed in Figure 4A, both poly($\mathbf{1}_1$-*co*-$\mathbf{2}_6$) and poly($\mathbf{1}_1$-*co*-$\mathbf{2}_{10}$) showed a strong UV−vis absorption at about 350 nm, indicating that both the copolymers took helical conformations. However, the maximum wavelengthes are a little different. For poly($\mathbf{1}_1$-*co*-$\mathbf{2}_6$), the UV peak appeared at 355 nm, while for poly($\mathbf{1}_1$-*co*-$\mathbf{2}_{10}$), the peak appeared at 350 nm. This variation results from the different maximum UV−vis absorption wavelength of poly-**1** (λ_{max}, 390 nm) and poly-**2** (λ_{max}, 350 nm) and also depends on the monomer feed ratios of the two monomers. In the CD spectra in Figure 4B, both the copolymers showed intense CD signals at the positions almost completely corresponding to the UV−vis absorption peaks. According to the UV−vis absorption peaks and CD effects of the copolymers and referring to the previous investigations on helical polyacetylenes,[10−12] it is indicated that both poly($\mathbf{1}_1$-*co*-$\mathbf{2}_6$) and poly($\mathbf{1}_1$-*co*-$\mathbf{2}_{10}$) formed helices under the examined conditions, and particularly important, both of them exhibited optical activities due to the predominantly one-handed screw sense. This is also in agreement with the large specific rotations mentioned above. Moreover, when the copolymers were subjected to UV−vis and CD analyses at varied temperatures, the strength of the peaks hardly changed upon enhancing temperature from 20 up to 60 °C. It is hence

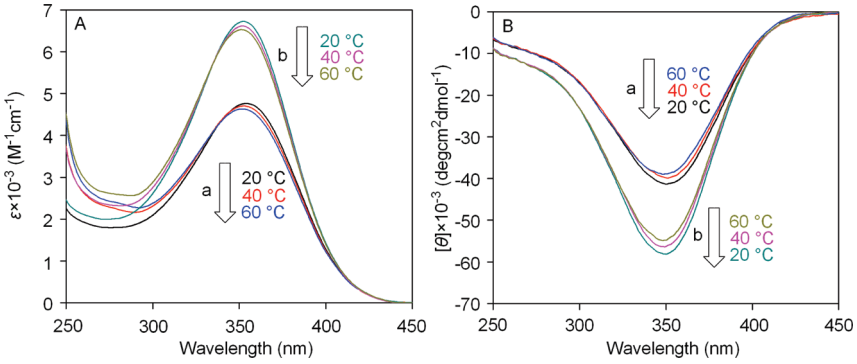

Figure 4. (A) UV−vis and (B) CD spectra of the macroinitiators (a) poly($\mathbf{1}_1$-*co*-$\mathbf{2}_6$) and (b) poly($\mathbf{1}_1$-*co*-$\mathbf{2}_{10}$) measured at varied temperatures in $CHCl_3$ (*c*, 0.1 mM).

Table 2. ATRP Reaction of DMAEMA Using Poly($\mathbf{1}_1$-*co*-$\mathbf{2}_6$) and Poly($\mathbf{1}_1$-*co*-$\mathbf{2}_{10}$) as Macroinitiators[a]

polymer brushes	yield (%)	time (h)	$M_{n,GPC}$[b]	M_w/M_n[b]	$M_{n,thr}$[c]	$M_{n,NMR}$[d]	$[\alpha]_D$ (deg)[e]	*g*-value[f]
poly($\mathbf{1}_1$-*co*-$\mathbf{2}_6$)-*g*-PDMAEMA2	g	2	12 400	1.82	g	g	g	g
poly($\mathbf{1}_1$-*co*-$\mathbf{2}_6$)-*g*-PDMAEMA4	g	4	18 300	1.67	g	g	g	g
poly($\mathbf{1}_1$-*co*-$\mathbf{2}_6$)-*g*-PDMAEMA8	77	8	21 100	1.66	29 100	28 100	−493	−2.49
poly($\mathbf{1}_1$-*co*-$\mathbf{2}_{10}$)-*g*-PDMAEMA	91	8	39 000	1.66	41 500	41 700	−1182	−2.55

[a] [DMAEMA]/[initiator]/[CuBr]/[HMTETA], 150/1/1/1.2, in mol; polymerization temperature, 60 °C; solvent, $CH_3OH/THF/H_2O$ = 1.5/3.5/0.5, in mL; [initiator] was calculated based on the molecular weight of **M1**. [b] Measured by GPC, using polystyrene as the standard and THF as eluent. [c] Theoretical value, $M_{n,thr}$ = ([DMAEMA]/[initiator]) × M_{DMAEMA} × yield % + $M_{n,initiator}$. [d] $M_{n,NMR} = (S_k/2S_{a'}) \times M_{DMAEMA} \times M_{n,initiator}/(M_{\mathbf{M1}} + ([\mathbf{M2}]/[\mathbf{M1}]) \times M_{\mathbf{M2}}) + M_{n,initiator}$, obtained by ^{1}H NMR analysis, where $S_k/2S_{a'}$ represents the average number of DMAEMA unit in one side chain and $M_{n,initiator}$ the number-average molecular weight of the macroinitiators; M_{DMAEMA}, $M_{\mathbf{M1}}$, and $M_{\mathbf{M2}}$ represent the molar mass of DMAEMA, **M1**, and **M2**, respectively. [e] Measured by polarimeter in $CHCl_3$ at room temperature (*c* = 0.085−0.1 g/dL). [f] *g*-value = $\Delta\varepsilon/\varepsilon$, in which $\Delta\varepsilon = [\theta]/3298$, temperature = 20 °C. The data of $\Delta\varepsilon$ and $[\theta]$ were based on Figure 5. [g] Not determined.

revealed that the helical structures of the copolymers were stable against heat in the examined temperature range.

Preparation of Amphiphilic Polymer Brushes via ATRP. The α-bromoisobutyryl groups in the helical copolymers prepared above rendered possibilities to perform ATRP, by which amphiphilic polymer brushes can be expected. Accordingly, ATRP of DMAEMA was carried out by using poly($\mathbf{1}_1$-*co*-$\mathbf{2}_6$) or poly($\mathbf{1}_1$-*co*-$\mathbf{2}_{10}$) as a macroinitiator and CuBr/HMTETA as catalyst/ligand at 60 °C in the mixture of CH_3OH, THF, and H_2O. It should be mentioned here that such a mixture solvent was chosen because of its good ability to dissolve the macroinitiator, monomer, catalyst, and the produced polymer. The polymerization took place smoothly and the viscosity of the reaction mixture appeared to increase with polymerization. In order to confirm the living feature of the present polymerization system, samples were taken from the reaction mixture to determine the molecular weight at different time intervals. After removal of the copper complex by passing the diluted polymer solutions in THF through an activated basic aluminum oxide column, the polymer brush was obtained as a yellow solid by precipitation in excess *n*-hexane. Then, the obtained polymers were subjected to GPC, and the relevant results are listed in Table 2 and the GPC traces are shown in Figure 2.

As can be seen in Figure 2, the molecular weights of poly($\mathbf{1}_1$-*co*-$\mathbf{2}_6$)-*g*-PDMAEMA increased with polymerization time while the molecular weight distributions decreased from 1.82 to 1.66. It should be pointed out that the molecular weight distributions were larger than 1.5 since the macroinitiators were not prepared via living catalytic polymerization. After ATRP, the molecular weights of the polymer brushes shifted to higher molecular weight positions with the elongation of polymerization, as seen in Figure 2. In addition, all the GPC traces of the polymer brushes were found to be unimodal without any trace of the unreacted macroinitiators, indicating that almost all the macroinitiators were converted to the corresponding polymer brushes.

To further verify the formation of polymer brushes, ^{1}H NMR spectra of poly($\mathbf{1}_1$-*co*-$\mathbf{2}_6$)-*g*-PDMAEMA8 and poly($\mathbf{1}_1$-*co*-$\mathbf{2}_{10}$)-*g*-PDMAEMA were measured and the relevant results are presented in Figure 1C,E. The signal located at a chemical shift of 2.55 ppm is associated with the methylene protons (l, N−CH_2) of the PDMAEMA side chains, and the peak at 2.26 ppm is attributable to the methylene protons (m, N−CH_3) in PDMAEMA chains. The integration area ratio (1:2.99 in poly($\mathbf{1}_1$-*co*-$\mathbf{2}_6$)-*g*-PDMAEMA8 and 1:3.06 in poly($\mathbf{1}_1$-*co*-$\mathbf{2}_{10}$)-*g*-PDMAEMA) of these protons was in good agreement with the theoretical ratio (1:3) of the corresponding protons, identifying the structures of the polymer brushes. Moreover, the chemical shifts at δ = 4.03 ppm reflect the methylene protons (k, CH_2−O−C═O) adjacent to the oxygen moieties of the ester linkages. The chemical shift associated with the olefinic protons (a′, −C═CH−) of is about 6.10 ppm. By comparing the integral intensity of the two peaks (k/2a′), the average polymerization degree (DP_n) of DMAEMA can be determined by $DP_n = S_k/2S_{a'}$. The average number (N_P) of PDMAEMA side chains is calculated by $N_P = M_{n,initiator}/(M_{\mathbf{M1}} + ([\mathbf{M2}]/[\mathbf{M1}])M_{\mathbf{M2}})$. Thus, the number-average molecular weight of the polymer brushes can be further determined according to $M_{n,NMR} = (S_k/2S_{a'})M_{DMAEMA}M_{n,initiator}/(M_{\mathbf{M1}} + ([\mathbf{M2}]/[\mathbf{M1}])M_{\mathbf{M2}}) + M_{n,initiator}$. In addition, the theoretical value of the molecular weight was calculated according to the following formula $M_{n,thr}$ = ([DMAEMA]/[initiator])M_{DMAEMA} × yield % + $M_{n,initiator}$. The calculation results are summarized in Table 2. It can be seen that the values of $M_{n,NMR}$ were nearly equal to those of $M_{n,thr}$. Nonetheless, the values of $M_{n,GPC}$ were a little lower than the corresponding $M_{n,NMR}$ and $M_{n,thr}$. This is due to the adsorption of PDMAEMA onto the GPC column to some extent, thus resulting in an increase in

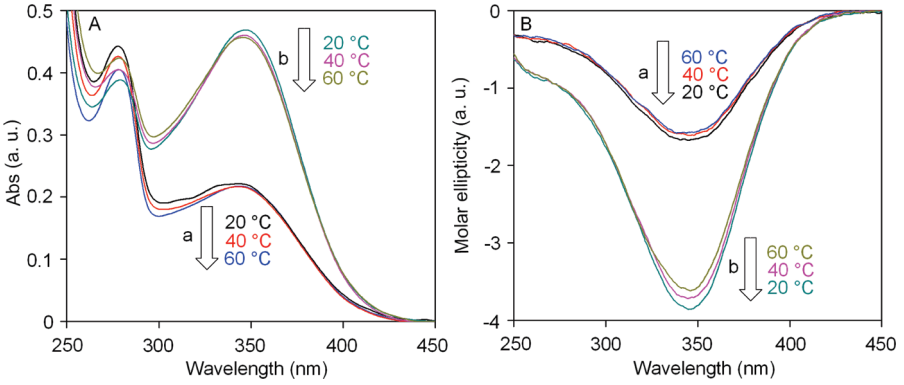

Figure 5. (A) UV−vis and (B) CD spectra of the polymer brushes (a) poly($\mathbf{1}_1$-*co*-$\mathbf{2}_6$)-*g*-PDMAEMA8 and (b) poly($\mathbf{1}_1$-*co*-$\mathbf{2}_{10}$)-*g*-PDMAEMA measured at varied temperatures in $CHCl_3$ ($c \sim 0.1$ mM).

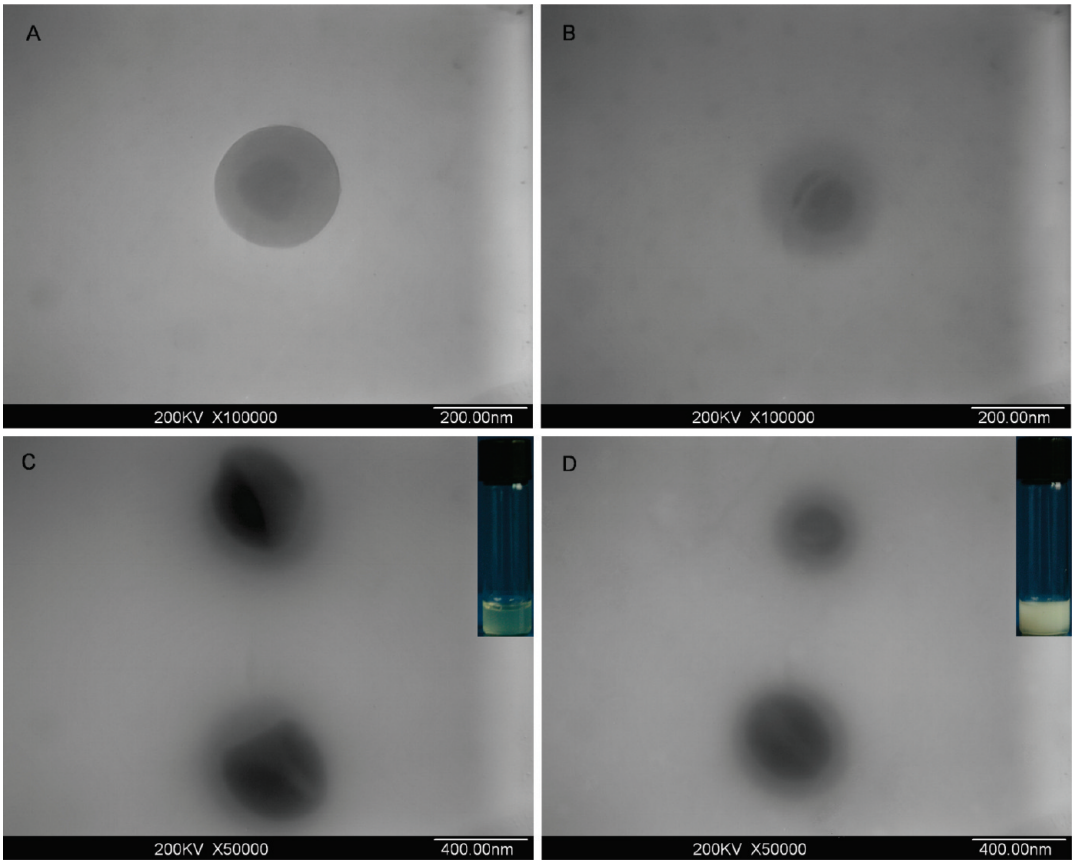

Figure 6. TEM images of the self-assembled core/shell nanoparticles from (A) poly($\mathbf{1}_1$-*co*-$\mathbf{2}_6$)-*g*-PDMAEMA8 at 25 °C, (B) poly($\mathbf{1}_1$-*co*-$\mathbf{2}_6$)-*g*-PDMAEMA8 at 60 °C, (C) poly($\mathbf{1}_1$-*co*-$\mathbf{2}_{10}$)-*g*-PDMAEMA at 25 °C, and (D) poly($\mathbf{1}_1$-*co*-$\mathbf{2}_{10}$)-*g*-PDMAEMA at 60 °C with a concentration of 10 mg/mL in THF/water (1/10, vol). The insets present the corresponding self-assembled systems of poly($\mathbf{1}_1$-*co*-$\mathbf{2}_{10}$)-*g*-PDMAEMA at 25 °C (in C) and at 60 °C (in D).

retention time and further leading to lower detected molecular weight than expected.[19]

Optical Activities of the Polymer Brushes. As can be seen in Figure 5, both poly($\mathbf{1}_1$-*co*-$\mathbf{2}_6$)-*g*-PDMAEMA8 and poly($\mathbf{1}_1$-*co*-$\mathbf{2}_{10}$)-*g*-PDMAEMA showed UV−vis absorptions and CD signals around 350 nm, clearly demonstrating the helical structures remaining in the polymer brushes. However, the UV−vis peaks and CD signals showed a blue shift when compared to the corresponding macroinitiators. This phenomenon is similar to our earlier investigations on the substituted polyacetylene emulsions.[13−15] The PDMAEMA side chains probably underwent inter- and intramolecular association due to their identical nature. This situation would enable the polymer backbones to be more packed and the effective conjugated length be shorter, by which a blue shift occurred. The intensities of the UV−vis peaks and CD signals in the polymer brushes were somewhat lower than those in the corresponding macroinitiators. Both poly($\mathbf{1}_1$-*co*-$\mathbf{2}_6$)-*g*-PDMAEMA8 and poly($\mathbf{1}_1$-*co*-$\mathbf{2}_{10}$)-*g*-PDMAEMA showed considerable specific rotations, as listed in Table 2, demonstrating that the polymer brushes were also optically active. Moreover, the optical activity of the polymer brushes was higher when more **M2** was used, as can be seen in the optical rotations and in the CD spectra. Nevertheless, the specific rotations of polymer brushes were lower than those of the corresponding macroinitiators. The aforementioned decreases

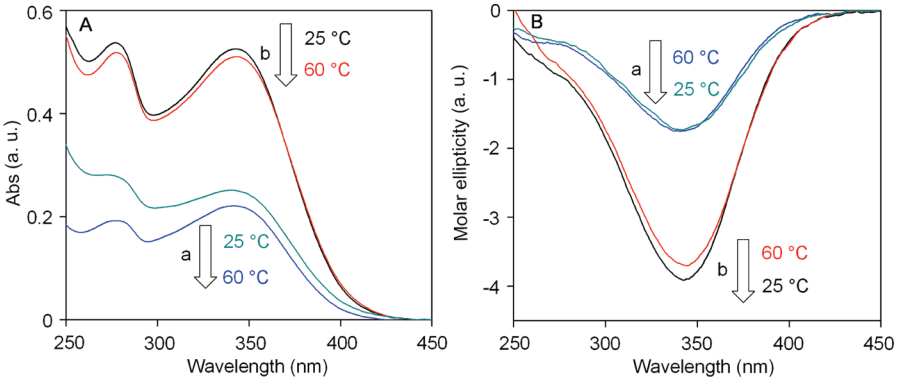

Figure 7. (A) UV−vis and (B) CD spectra of the micelle solutions from (a) poly($\mathbf{1}_1$-*co*-$\mathbf{2}_6$)-*g*-PDMAEMA8 and (b) poly($\mathbf{1}_1$-*co*-$\mathbf{2}_{10}$)-*g*-PDMAEMA measured at varied temperatures. The samples were diluted 500 times with deionized water before measurement ($c \sim 0.1$ mM).

in specific rotations, UV−vis absorption, and CD intensities should be originated in the decreased helical polymer contents after the incorporation of PDMAEMA side chains. Furthermore, the intensities of UV−vis absorptions and CD signals of the polymer brushes measured at different temperatures exhibited only slight difference, reflecting that the helical structures in the polymer brushes were also stable in the temperature range from 20 to 60 °C. In addition, the Kuhn dissymmetry factor[20] (*g*-value, in Tables 1 and 2) was calculated to make a quantitative comparison among the polymers. It can be observed that poly($\mathbf{1}_1$-*co*-$\mathbf{2}_6$) and poly($\mathbf{1}_1$-*co*-$\mathbf{2}_{10}$) exhibited similar *g*-values, which kept almost unchanged even after the incorporation of PDMAEMA side chains, indicating that both the macroinitiators and polymer brushes possessed stable preferential helical screw sense.

Self-Assembly of the Amphiphilic Polymer Brushes. The as-prepared poly($\mathbf{1}_1$-*co*-$\mathbf{2}_6$)-*g*-PDMAEMA and poly($\mathbf{1}_1$-*co*-$\mathbf{2}_{10}$)-*g*-PDMAEMA feature amphiphilic structures consisting of hydrophobic poly(*N*-propargylamide) main chains and hydrophilic PDMAEMA side chains, so they in principle can undergo self-assembly in appropriate solvents to form nanostructures. We found water/THF is an ideal solvent system for performing the self-assembly. The morphology of the self-assembly products from poly($\mathbf{1}_1$-*co*-$\mathbf{2}_6$)-*g*-PDMAEMA8 and poly($\mathbf{1}_1$-*co*-$\mathbf{2}_{10}$)-*g*-PDMAEMA were visualized by TEM, as shown in Figure 6.

Core/shell structured nanoparticles are observed in the two cases, in both of which the shells can be clearly distinguished from the cores (Figure 6). We also found that when more **M2** was incorporated in the polymer brush (poly($\mathbf{1}_1$-*co*-$\mathbf{2}_{10}$)-*g*-PDMAEMA), the shell of the particle became thinner (for poly($\mathbf{1}_1$-*co*-$\mathbf{2}_{10}$)-*g*-PDMAEMA, 67 nm shell in 420 nm core/shell particle, and for poly($\mathbf{1}_1$-*co*-$\mathbf{2}_6$)-*g*-PDMAEMA8, 87 nm shell in 270 nm core/shell particle; the data were calculated from Figure 6). This is originated from the lower graft density of poly($\mathbf{1}_1$-*co*-$\mathbf{2}_{10}$)-*g*-PDMAEMA compared to poly($\mathbf{1}_1$-*co*-$\mathbf{2}_6$)-*g*-PDMAEMA8. As a typical representative, the average diameter of the core/shell nanoparticles from poly($\mathbf{1}_1$-*co*-$\mathbf{2}_{10}$)-*g*-PDMAEMA at 25 °C was determined as 354.6 nm. More interestingly, we found that the average diameter of the nanoparticles decreased to 299.8 nm when measured at 60 °C. The diameter change was reversible. That is, when the temperature decreased to 25 °C, the measured diameter of the nanoparticles increased to 357.4 nm. PDMAEMA is well-known to be a thermosensitive polymer showing a lower critical solution temperature (LCST) in the range 32−46 °C.[21] Hence, it can be supposed that the PDMAEMA shells of the self-assembled nanoparticles would become thinner at a higher temperature than LCST and result in a decrease in average diameter. In addition, the self-assembled core/shell nanoparticles from poly($\mathbf{1}_1$-*co*-$\mathbf{2}_{10}$)-*g*-PDMAEMA at 25 °C (the inset in Figure 6C) was transparent while the corresponding system at 60 °C (the inset in Figure 6D) was almost opaque, providing evidence for the consideration that the self-assembly core/shell nanoparticles are thermoresponsive.

UV−vis and CD spectra of the polymer brushes after self-assembly are presented in Figure 7. The spectra are found to be quite similar to those of the corresponding polymer brushes measured in chloroform, which are illustrated in Figure 5. Both of the self-assemblies showed UV−vis absorptions and intensive CD signals at ca. 350 nm, and blue shifts also occurred in the spectra, when compared to those in Figure 4. It is thus concluded that the helical structures kept well and the self-assembled core/shell nanoparticles were also optically active. More importantly, when the samples were measured at a high temperature up to 60 °C, the UV−vis absorptions and CD signals could be observed still and their strengths changed little, demonstrating the high thermostability of the helical structures and optical activities in the core/shell nanoparticles formed via self-assembly.

Conclusions

A novel *N*-propargylamide monomer containing in particular designed α-bromoisobutyryl group was first synthesized and then copolymerized with another *N*-propargylamide monomer, successfully providing optically active helical copolymers. Such helical copolymers were further used as macroinitiators for ATRP of DMAEMA to produce amphiphilic optically active polymer brushes consisting of helical poly(*N*-propargylamide)s main chains and thermosensitive PDMAEMA side chains. UV−vis and CD spectroscopy measurements and specific rotations demonstrated that the polymer brushes possessed considerable optical activity. More importantly, the novel polymer brushes can self-assemble to provide core/shell nanoparticles with optically active cores (helical polyacetylene) and thermoresponsive shells (PDMAEMA). Such nanoparticles also showed considerable optical activities, derived from the helical structures forming the cores. The as-prepared polymer brushes and core/shell nanoparticles are expected to find potential applications in chiral materials, stimulus-responsive materials, etc.

Acknowledgment. This work was supported by the "Program for New Century Excellent Talents in University" (NCET-06-0096), "the National Science Foundation of China" (20974007), the "Program for Changjiang Scholars and Innovative Research Team in University" (PCSIRT, IRT0706), and the "Major Project for Polymer Chemistry and Physics Subject Construction from Beijing Municipal Education Commission (BMEC)".

We thank Professor Fujian Xu for helpful discussions on ATRP reaction.

References and Notes

(1) (a) Sheiko, S. S.; Sumerlin, B. S.; Matyjaszewski, K. *Prog. Polym. Sci.* **2008**, *33*, 759. (b) Zhang, M.; Müller, A. H. E. *J. Polym. Sci., Part A: Polym. Chem.* **2005**, *43*, 3461. (c) Hadjichristidis, N.; Pitsikalis, M.; Iatrou, H.; Pispas, S. *Macromol. Rapid Commun.* **2003**, *24*, 979. (d) Ito, K.; Kawaguchi, S. *Adv. Polym. Sci.* **1999**, *142*, 129.

(2) (a) Xu, Y.; Bolisetty, S.; Ballauff, M.; Müller, A. H. E. *J. Am. Chem. Soc.* **2009**, *131*, 1640. (b) Xu, Y.; Bolisetty, S.; Drechsler, M.; Fang, B.; Yuan, J.; Harnau, L.; Ballauff, M.; Müller, A. H. E. *Soft Matter* **2009**, *5*, 379. (c) Xu, Y.; Bolisetty, S.; Drechsler, M.; Fang, B.; Yuan, J.; Ballauff, M.; Müller, A. H. E. *Polymer* **2008**, *49*, 3957. (d) Rühe, J.; Ballauff, M.; Biesalski, M.; Dziezok, P.; Gröhn, F.; Johannsmann, D.; Houbenov, N.; Hugenberg, N.; Konradi, R.; Minko, S.; Motornov, M.; Netz, R. R.; Schmidt, M.; Seidel, C.; Stamm, M.; Stephan, T.; Usov, D.; Zhang, H. *Adv. Polym. Sci.* **2004**, *165*, 79. (e) Li, C.; Gunari, N.; Fischer, K.; Janshoff, A.; Schmidt, M. *Angew. Chem., Int. Ed.* **2004**, *43*, 1101. (f) Djalali, R.; Li, S. Y.; Schmidt, M. *Macromolecules* **2002**, *35*, 4282.

(3) (a) Gao, H.; Matyjaszewski, K. *J. Am. Chem. Soc.* **2007**, *129*, 6633. (b) Börner, H. G.; Beers, K.; Matyjaszewski, K.; Sheiko, S. S.; Möller, M. *Macromolecules* **2001**, *34*, 4375. (c) Beers, K. L.; Gaynor, S. G.; Matyjaszewski, K.; Sheiko, S. S.; Möller, M. *Macromolecules* **1998**, *31*, 9413. (d) Dziezok, P.; Fischer, K.; Schmidt, M.; Sheiko, S. S.; Möller, M. *Angew. Chem., Int. Ed.* **1997**, *36*, 2812.

(4) (a) Müllner, M.; Yuan, J.; Weiss, S.; Walther, A.; Förtsch, M.; Drechsler, M.; Müller, A. H. E. *J. Am. Chem. Soc.* **2010**, *132*, 16587. (b) Xu, L. Q.; Wan, D.; Gong, H. F.; Neoh, K. G.; Kang, E. T.; Fu, G. D. *Langmuir* **2010**, *26*, 15376. (c) Yuan, J.; Lu, Y.; Schacher, F.; Lunkenbein, T.; Weiss, S.; Schmalz, H.; Müller, A. H. E. *Chem. Mater.* **2009**, *21*, 4146. (d) Yuan, J.; Xu, Y.; Walther, A.; Bolisetty, S.; Schumacher, M.; Schmalz, H.; Ballauff, M.; Müller, A. H. E. *Nature Mater.* **2008**, *7*, 718. (e) Yuan, J.; Schmalz, H.; Xu, Y.; Miyajima, N.; Drechsler, M.; Möller, M. W.; Schacher, F.; Müller, A. H. E. *Adv. Mater.* **2008**, *20*, 947. (f) Xie, M.; Dang, J.; Han, H.; Wang, W.; Liu, J.; He, X.; Zhang, Y. *Macromolecules* **2008**, *41*, 9004. (g) Zhang, B.; Gröhn, F.; Pedersen, J. S.; Fischer, K.; Schmidt, M. *Macromolecules* **2006**, *39*, 8440. (h) Hu, D.; Cheng, Z.; Zhu, J.; Zhu, X. *Polymer* **2005**, *46*, 7563. (i) Edmondson, A.; Osborne, V. L.; Huck, W. T. S. *Chem. Soc. Rev.* **2004**, *33*, 14.

(5) (a) Nguyen, L. T. T.; Musser, A. J.; Vorenkamp, E. J.; Polushkin, E.; Brinke, G.; Schouten, A. J. *Langmuir* **2010**, *26*, 14073. (b) Yang, C. T.; Wang, Y.; Chang, Y. C. *Biomacromolecules* **2010**, *11*, 1308. (c) Engler, A. C.; Lee, H.; Hammond, P. T. *Angew. Chem., Int. Ed.* **2009**, *48*, 9334. (d) Yang, C. H.; Wang, Y.; Yu, S.; Chang, Y. C. *Biomacromolecules* **2009**, *10*, 58. (e) Gunari, N.; Cong, Y.; Zhang, B.; Fischer, K.; Janshoff, A.; Schmidt, M. *Macromol. Rapid Commun.* **2008**, *29*, 821. (f) Lim, E.; Tu, G.; Schwartz, E.; Cornelissen, J. J. L. M.; Rowen, A. E.; Nolte, R. J. M.; Huck, W. T. S. *Macromolecules* **2008**, *41*, 1945.

(6) (a) Qin, Z.; Chen, Y.; Zhou, W.; He, X.; Bai, F.; Wan, M. *Eur. Polym. J.* **2008**, *44*, 3732. (b) Zhang, W.; Shiotsuki, M.; Masuda, T. *Macromol. Rapid Commun.* **2007**, *28*, 1115. (c) Zhang, W.; Shiotsuki, M.; Masuda, T. *Polymer* **2007**, *48*, 2548. (d) Zhang, W.; Shiotsuki, M.; Masuda, T.; Kumaki, J.; Yashima, E. *Macromolecules* **2007**, *40*, 178. (e) Maeda, K.; Kamiya, N.; Yashima, E. *Chem.—Eur. J.* **2004**, *10*, 4000.

(7) (a) Kong, X. X.; Kulkarni, A. P.; Jenekhe, S. A. *Macromolecules* **2003**, *36*, 8992. (b) Fungo, F.; Jenekhe, S. A.; Bard, A. J. *Chem. Mater.* **2003**, *15*, 1264. (c) Babel, A.; Jenekhe, S. A. *Adv. Mater.* **2002**, *14*, 371.

(8) (a) Shirakawa, H. *Angew. Chem., Int. Ed.* **2001**, *40*, 2574. (b) McDiarmid, A. G. *Angew. Chem., Int. Ed.* **2001**, *40*, 2581. (c) Heeger, A. J. *Angew. Chem., Int. Ed.* **2001**, *40*, 2591.

(9) (a) Yashima, E.; Maeda, K.; Iida, H.; Furusho, Y.; Nagai, K. *Chem. Rev.* **2009**, *109*, 6102. (b) Percec, V.; Rudick, J. G.; Peterca, M.; Heiney, P. A. *J. Am. Chem. Soc.* **2008**, *130*, 7503. (c) Fujiki, M. *Top. Curr. Chem.* **2008**, *284*, 119. (d) Masuda, T. *J. Polym. Chem., Part A: Polym. Chem.* **2007**, *45*, 165. (e) Sinkeldam, R. W.; van Houtem, M. H. C. J.; Pieterse, K.; Vekemans, J. A. J. M.; Meijer, E. W. *Chem.—Eur. J.* **2006**, *12*, 6129. (f) Lam, J. E. Y.; Tang, B. Z. *Acc. Chem. Res.* **2005**, *38*, 745. (g) Aoki, T.; Kaneko, T.; Maruyama, N.; Sumi, A.; Takahashi, M.; Sato, T.; Teraguchi, M. *J. Am. Chem. Soc.* **2003**, *125*, 6346. (h) Nakano, T.; Okamoto, Y. *Chem. Rev.* **2001**, *101*, 4013. (i) Mayer, S.; Zentel, R. *Prog. Polym. Sci.* **2001**, *26*, 1973. (j) Green, M. M.; Park, J. W.; Sato, T.; Teramoto, A.; Lifson, S.; Selinger, R. L. B.; Selinger, J. V. *Angew. Chem., Int. Ed.* **1999**, *38*, 3138. (k) Rowan, A. E.; Nolte, R. J. M. *Angew. Chem., Int. Ed.* **1998**, *37*, 63. (l) Pu, L. *Acta Polym.* **1997**, *48*, 116.

(10) (a) Ding, L.; Jiao, X. F.; Deng, J. P.; Zhao, W. G.; Yang, W. T. *Macromol. Rapid Commun.* **2009**, *30*, 120. (b) Deng, J. P.; Zhao, W. G.; Wang, J. M.; Zhang, Z. G.; Yang, W. T. *Macromol. Chem. Phys.* **2007**, *208*, 218. (c) Deng, J. P.; Tabei, J.; Shiotsuki, M.; Sanda, F.; Masuda, T. *Macromolecules* **2004**, *37*, 9715.

(11) (a) Zhang, Z. G.; Deng, J. P.; Zhao, W. G.; Wang, J. M.; Yang, W. T. *J. Polym. Sci., Part A: Polym. Chem.* **2007**, *45*, 500. (b) Deng, J. P.; Tabei, J.; Shiotsuki, M.; Sanda, F.; Masuda, T. *Macromolecules* **2004**, *37*, 5538.

(12) (a) Luo, X. F.; Chang, J.; Deng, J. P.; Yang, W. T. *React. Funct. Polym.* **2010**, *70*, 116. (b) Deng, J. P.; Luo, X. F.; Zhao, W. G.; Yang, W. T. *J. Polym. Sci., Part A: Polym. Chem.* **2008**, *46*, 4112.

(13) (a) Luo, X. F.; Li, L.; Deng, J. P.; Guo, T. T.; Yang, W. T. *Chem. Commun.* **2010**, *46*, 2745. (b) Luo, X. F.; Kang, N. W.; Li, L.; Deng, J. P.; Yang, W. T. *J. Polym. Sci., Part A: Polym. Chem.* **2010**, *48*, 1661. (c) Deng, J. P.; Chen, B.; Luo, X. F.; Yang, W. T. *Macromolecules* **2009**, *42*, 933.

(14) (a) Chen, B.; Deng, J. P.; Liu, X. Q.; Yang, W. T. *Macromolecules* **2010**, *43*, 3177. (b) Chen, B.; Deng, J. P.; Tong, L. Y.; Yang, W. T. *Macromolecules* **2010**, DOI: 10.1021/ma102157e.(c) Luo, X. F.; Liu, X. Q.; Chen, B.; Deng, J. P.; Yang, W. T. *J. Polym. Sci., Part A: Polym. Chem.* **2010**, *48*, 5611.

(15) Zhang, Y. Y.; Luo, X. F.; Deng, J. P. Yang, W. T. *Macromol. Chem. Phys.* **2010**, DOI: 10.1002/macp201000606.

(16) Schrock, R. R.; Osborn, J. A. *Inorg. Chem.* **1970**, *10*, 2339.

(17) Tabei, J.; Nomura, R.; Masuda, T. *Macromolecules* **2002**, *35*, 5405.

(18) Xu, F. J.; Zhang, Z. X.; Ping, Y.; Li, J.; Kang, E. T.; Neoh, K. G. *Biomacromolecules* **2009**, *10*, 285.

(19) (a) Creutz, S.; Teyssié, P.; Jérôme, R. *Macromolecules* **1997**, *30*, 6. (b) Baines, F. L.; Billingham, N. C.; Armes, S. P. *Macromolecules* **1996**, *29*, 3416.

(20) Fujiki, M. *Macromol. Rapid Commun.* **2001**, *22*, 539.

(21) Bütün, V.; Armes, S. P.; Billingham, N. C. *Polymer* **2001**, *42*, 5993.